

## Size effects in the phase change properties of sub-10 nm PCM clusters

R. Morel<sup>1</sup>, G. E. Ghezzi<sup>2,4</sup>, A. Brenac<sup>1</sup>, N. Boudet<sup>3</sup>, F. Fillot<sup>2</sup>, P. Noé<sup>2</sup>, S. Maîtrejean<sup>2</sup>, M. Audier<sup>4</sup>, and F. Hippert<sup>4,5</sup>

<sup>1</sup>INAC/SP2M et Université Joseph Fourier, CEA Grenoble, 17 rue des Martyrs, Grenoble, France

<sup>2</sup>CEA, LETI, MINATEC Campus, 17 rue des Martyrs, 38054 Grenoble, France

<sup>3</sup>Institut Néel, CNRS/UJF, 25 rue des Martyrs, BP 166, 38042 Grenoble, France

<sup>4</sup>Laboratoire des Matériaux et du Génie Physique (Grenoble-INP, CNRS), MINATEC, 3 Parvis L. Néel, Grenoble, France

<sup>5</sup>LNCMI, CNRS, 25 rue des Martyrs, BP 166, 38042 Grenoble, France

robert.morel@cea.fr.

### ABSTRACT

Due to the large difference in the electrical properties for the amorphous and crystalline phases, Phase Change Materials are good candidates for application in non-volatile memories. However, viable application calls for bit size less than a few tens of nanometers. This reduction in the size of the active element opens a number of questions regarding the scalability of PCM, the first one being their ability to crystallize at ultimate dimensions and the size dependence of the crystallization temperature  $T_x$ .

In this paper we describe the use of a sputtering-gas aggregation technique for the growth of GST nanometric clusters with size below 10 nm, which has allowed for the study of phase transition in isolated amorphous particles. Despite the strong confinement and significant strain in the final structure, the crystallization is observed at temperature close to that of the bulk material.

**Key words:** GST clusters, size effects, crystallization temperature

### 1. INTRODUCTION

The unique properties displayed by Phase Change Materials (PCM) have allowed for the development of rewritable optical storage media. Due to the large difference in the electrical properties for the amorphous and crystalline phases, PCM are also good candidates for application in non-volatile memories. Viable PCRAM application calls for bit size of a few tens of nanometers, hence with bit volume two or three orders of magnitude smaller than that of optical storage media. This reduction in the size of the active element opens a number of questions regarding the scalability of PCM, the first one being their ability to crystallize at ultimate dimensions and the size dependence of the crystallization temperature  $T_x$ .

Many studies regarding the scalability of the PCM deal with the thickness dependence of the amorphous to crystalline phase transition in GST thin films [1, 2]. An increase in  $T_x$  is reported when the film thickness is reduced below 20 nm. In parallel with this change in  $T_x$ , the increase in the crystallization activation energy and the change in the Avrami coefficient suggest that the nucleation and growth mechanisms change by decreasing thickness [1].

The change in  $T_x$  can be explained with the help of the Zacharias model [3]. In this model, based on the free energy calculation for the homogeneous nucleation, an effective interfacial energy between the oxide capping layer and the surface of a growing crystallite can give rise to an exponential increase in  $T_x$  as the thickness is reduced, as experimentally reported [2]. Nevertheless, for a given

pair of PC material and cladding material the change in  $T_x$  with thickness is difficult to predict with this model alone.

On one hand, it is observed that different PC materials thin films capped with alumina behave very differently [2]: With the same capping, the increase in  $T_x$  at 2 nm is very large in  $\text{Ge}_2\text{Sb}_2\text{Te}_5$  (GST) – more than 200°C – while in GeSb it is less than 50°C, with a significant variation only below 3.5 nm. On the other hand, different cladding materials induce very different effects as has been shown for instance with the study of the effect of different dielectric materials on the crystallization mechanism of PC thin films [4].  $\text{Si}_3\text{N}_4$  and  $\text{Ta}_2\text{O}_5$  capped films show higher nucleation rates, while nucleation is inhibited in  $\text{SiO}_2$  capped sample, and ZnS and ZnS- $\text{SiO}_2$  capped samples show generation of nuclei even during the grain growth process. These variations are attributed to differences in the surface reactivity and chemical affinity of the film materials [4].

One key element regarding the scalability of the phase change transition that was considered only recently is the effect of the mechanical stress that is exerted on the PC thin film, both during the thermal cycling and at crystallization. Compared with usual dielectric material used for cladding, GST has a very high thermal coefficient: a thin film deposited on a substrate or inserted in a dielectric matrix is likely to suffer a significant compressive stress upon heating, while the 4.7% density increase at crystallization could on the other hand give rise to an even larger tensile stress [5]. Given this it would have been expected that a compressive stress on the amorphous phase would favor the crystalline phase change. However, recent papers show opposite results. For instance a compressive stress (240 MPa) in TiN-cladded GST thin film was shown to induce an increase in  $T_x$  as the thickness decreases, while a smaller compressive stress (58 MPa, with ZnS- $\text{SiO}_2$  cladding) gives rise to a small reduction in  $T_x$  [6]. A second recent report indicates that  $T_x$  for GST films increases as external compressive stress is applied, but also that it decreases under tensile stress, and that in both cases the span of the transition is widened [7]. Finally, in a third report, with larger compressive and tensile stress, it is shown that stresses have a large influence for the cubic to hexagonal transition temperature, and even suppress this transition for both compressive stress and tensile stress when the GST film thickness is thinner than 10 nm [8].

In a context where the study of size effects in phase change materials is needed to assess the ultimate limits for the scalability of devices, the usefulness of embedded nanometric clusters is twofold. First, compared with thin films the clusters provide a larger surface to volume ratio that should enhance the surface and interface properties with respect to their bulk properties. Second, the elastic properties of an ensemble of clusters in a matrix differ significantly from those of the thin films that have been studied up to now. In the latter case the fact that the stress is bi-axial, in the plane of the film, results in an intrinsically inhomogeneous strain which effect on the phase transition is difficult to anticipate. Even more important, the plastic relaxation in a PC material thin film, either in the amorphous phase or at the interface with the crystalline phase at the transition, gives rise to a very large stress relaxation [9]. On the opposite, with embedded nanometric clusters there are fewer mechanisms available for stress relief and the stress is more likely homogeneous, at least with spherical particles.

In this paper we describe the use of a sputtering-gas aggregation technique for the growth of GST nanometric clusters in the sub-10 nm size range, and the study of phase transition in isolated amorphous particles embedded in alumina. The amorphous to crystalline phase transition was measured with X ray diffraction spectroscopy, which also allowed for the measurement of the strain in the crystallized clusters.

## 2. EXPERIMENTS

The GST nanometric clusters are prepared using sputtering-gas phase condensation [10]. The cluster source consists in a magnetron sputtering head inserted in a liquid nitrogen-cooled tube, in which

particles grow from sputtered atoms collision in cold Ar buffer gas. Grown clusters are expelled from the source, into a high vacuum chamber, forming a beam which is directed onto a deposition stage. Additional sputtering heads are used for the deposition of GST thin films and  $\text{Al}_2\text{O}_3$ . The clusters size distribution – with a typical average size between 5 - 6 nm – is measured in situ by time of flight mass spectrometry (Fig. 1).

Two types of GST samples have been prepared in order to assess the crystallization temperature by X-ray diffraction (XRD) measurements. The GST clusters samples consist in multilayers of clusters and alumina deposited on Si (Figure 2), with 20 nm alumina thin film interspersed with four layers of GST clusters for a total equivalent thickness of 2 nm. The low clusters content has been chosen to avoid sintering effects during annealing: given the density and their lack of mobility upon deposition, most of the clusters are isolated and entirely embedded in the alumina matrix. In thin films samples the GST thickness was 10 nm, sandwiched between two 10 nm alumina layers. Both thin films and clusters compositions were measured with RBS and PIXE. The thin films content is Ge:Sb:Te = 23:24:53 ( $\pm 3$ ), very close to the  $\text{Ge}_2\text{Sb}_2\text{Te}_5 = 22:22:56$  target composition. Clusters composition is 28:27:45 ( $\pm 3$ ), which indicates a slight Te depletion as often reported for very thin films and clusters [2,11,12]. The GST clusters composition before and after annealing is found identical within experimental accuracy.

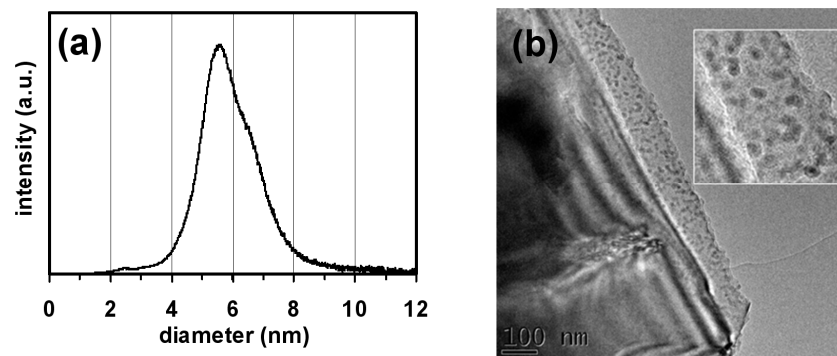


Figure 1. (a) GST clusters size distribution measured by time-of-flight spectrometry. (b) TEM image of a multilayer with GST clusters embedded in alumina.

### 3. RESULTS & DISCUSSION

Because the signal intensity recorded with in situ annealing is very low, a first set of clusters and thin film samples was annealed under vacuum at various temperatures prior to the X-ray measurement (ex situ samples). X-ray diffraction on those samples has been performed at room temperature. For a second set of clusters and thin films samples the X-ray diffraction spectra were recorded as a function of the temperature, during the annealing process (in situ samples). X-ray diffraction measurements were performed on the BM02 CRG-D2AM synchrotron radiation beamline (ESRF Grenoble, France) using a 2D CCD camera detector.

The 2D images obtained for the as-deposited GST film and clusters show no diffraction rings, which confirms that they are both amorphous. The 2D images for the 200°C ex situ annealed samples – after substrate signal subtraction – are shown at Figure 2. For the thin film the diffraction spectra clearly show a GST fcc cubic structure with texture, while for the clusters two rings corresponding to the (200) and (220) diffraction lines are seen. Due to the small amount of clusters and their very small size

the diffraction rings are faint and broadened, and only the two most intense diffraction lines are observed.

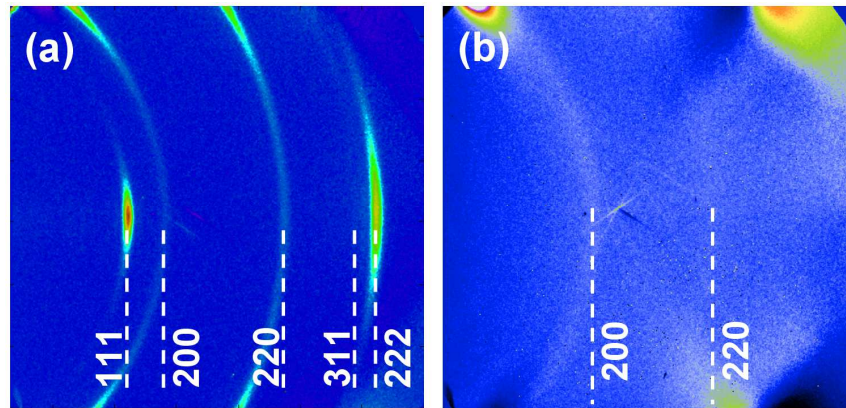


Figure 2. X ray diffraction spectra for GST thin film (a) and clusters (b) after annealing at 200°C. Diffraction lines are indexed relative to the GST bulk fcc phase.

Details on the measurements for the in situ annealed thin films and clusters are reported elsewhere [13]. The crystallization temperature in the thin films, as determined by the mid in the rise of the intensity of the diffraction peaks, is 155°C with a range of 20°C (Fig. 3). This value is similar to that of bulk GST as expected for a 10 nm film. The clusters crystallization begins at more or less the same temperature, but proceeds more slowly over a 50°C range with a  $T_x$  close to 180°C. This value for clusters is close to that of the thin film measured in a similar way, and lower than the reported value for 5 nm alumina-cladded GST thin films, with a  $T_x$  of more than 330°C.

The RT fcc lattice parameter for the 200°C ex situ annealed samples can be estimated from the different diffraction lines, as shown in Figure 4. For the thin film an uncertainty arises regarding the [222] peak position due to the [111] texture and the fact that the diffraction spectrum is recorded with constant angle of incidence. Nevertheless, the average value for the thin film lattice parameter is 0.601 +/- 0.001 nm. This value is in good agreement with the reported value for bulk GST, 0.60117(5) nm [5], indicating that the mechanical stress resulting from the thin film crystallization is relaxed. Due to the very high background noise the lattice parameter determination for the crystallized is less precise but the best estimates indicate a significantly larger lattice parameter, 0.611 nm +/- 0.002 nm, which represents a 1.7% tensile strain.

The extent of this strain is such that the stretched volume of the crystallized cluster is similar to that of the amorphous phase cluster prior to its crystallization. This is a striking difference with GST thin films where only 10% of the volume change at the phase transition transforms into elastic strain [9]. Here, the full extent of the tensile strain is observed in crystallized clusters. Also shown in Fig. 4 is the change in the lattice parameter for clusters annealed at 200°C, 300°C and 400°C, which are all in the cubic fcc phase. As can be observed the strain decreases with further annealing, although it is still present in clusters annealed at 400°C.

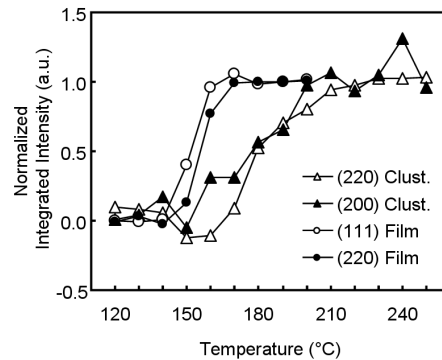


Figure 3. Normalized integrated intensities as a function of temperature for GST clusters (200) and (220) diffraction peaks, and GST film (111) and (220) diffraction peaks.

The fact that no relaxation occurs for isolated embedded GST clusters close to  $T_x$ , which on the other hand is very close to that of thin films, is an indication that the stress is not an impediment for the phase transition. This could be explained by noting that the elastic energy stored in crystallized clusters ( $\sim 50 \text{ MJ/m}^3$ ) is significantly lower than the driving force for the phase transition, which is about  $200 \text{ MJ/m}^3$  [14]. On the other hand, if one considers the stress on the embedded amorphous clusters prior to their crystallization, it is calculated that at  $155^\circ\text{C}$  the uniform stress on the amorphous cluster is of the order of 50-100 MPa [15, 16]. Contrary to what is observed with some thin films, in the case of clusters this stress positively contributes to the phase transition occurrence and counterbalances other possible interface effects, keeping  $T_x$  close to its bulk value.

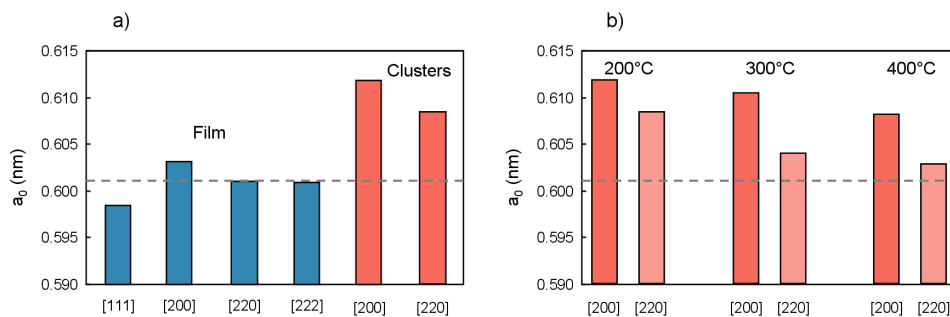


Figure 4. Cubic lattice parameter  $a_0$  calculated from different diffraction lines measured (a) for  $200^\circ\text{C}$  ex situ annealed thin film and clusters and (b) for clusters annealed at  $200^\circ\text{C}$ ,  $300^\circ\text{C}$  and  $400^\circ\text{C}$ . In both figures the dashed lines indicate the GST bulk lattice parameter.

#### 4. CONCLUSION

While previous reports on thin films indicate a large increase in  $T_x$  for thin films below 10 nm, due to either some interface interaction or stress effects, we measure in this report a transition temperature for 5-6 nm GST clusters embedded in alumina that is only  $30^\circ\text{C}$  above the bulk value. This temperature is the lowest observed for the GST crystallization in the sub-10 nm range, pointing to possible device application down to this length scale. Given the large strain observed in crystallized clusters we conclude that, contrary to thin films, no stress relaxation occurs at the transition despite

the large change in the density. This is a clear indication that, when no plastic relaxation is allowed, the amorphous to crystalline phase transition can withstand a large elastic stress, which calls for further study on the role of elastic stress on the phase change transition.

## REFERENCES

1. X. Wei, S. Luping, Z. Chong, C. T. Rong, and L. H. Koon, *Jpn. J. Appl. Phys.* **46** (2007) 2211
2. S. Raoux, J. L. Jordan-Sweet, and A. J. Kellock, *J. Appl. Phys.* **103** (2008) 114310
3. M. Zacharias and P. Streitenberger, *Phys. Rev. B* **62** (2000) 8391
4. N. Ohshima, *J. Appl. Phys.* **79** (1996) 8357
5. T. Nonaka, G. Ohbayashia, Y. Toriumib, Y. Morib, H. Hashimoto, *Thin Solid Films* **370** (2000) 258
6. R. E. Simpson, M. Krbal, P. Fons, A. V. Kolobov, J. Tominaga, T. Uruga, and H. Tanida, *Nano Letters* **10** (2009) 414419
7. Y. Du, Y. Kan, X. Lu, Y. Liu, H. Bo, W. Cai, D. Hu, F. Huang, and J. Zhu, *Phys. Status Solidi RRL* (2013)
8. H.-Y. Cheng, S. Raoux, C.-W. Cheng, and J. L. Jordan-Sweet, *MRS Spring Meeting 2012* (2012)
9. T. P. Leervad Pedersen, J. Kalb, W. K. Njoroge, D. Wamwangi, M. Wuttig, and F. Spaepen, *Appl. Phys. Lett.* **79** (2001) 3597
10. R. Morel, A. Brenac, P. Bayle-Guillemaud, C. Portemont, and F. La Rizza, *Eur. Phys. J. D* **24** (2003) 287
11. S. Raoux, C. T. Rettner, J. L. Jordan-Sweet, A. J. Kellock, T. Topuria, P. M. Rice, and D. C. Miller, *J. Appl. Phys.* **102** (2007) 094305
12. H. R. Yoon, W. Jo, E. H. Lee, J. H. Lee, M. Kim, K. Y. Lee, and Y. Khang, *J. Non-Cryst. Solids* **351** (2005) 3430; H. R. Yoon, W. Jo, E. Cho, S. Yoon, and M. Kim, *J. Non-Cryst. Solids* **352** (2006) 3757
13. G. E. Ghezzi, R. Morel, A. Brenac, N. Boudet, M. Audier, F. Fillot, S. Maitrejean, and F. Hippert, *J. Appl. Phys.* **101** (2012) 233113
14. J. A. Kalb, M. Wuttig, and F. Spaepen, *J. Mater. Res.* **22** (2007) 748
15. A. Marmier, K. Kohary, and C. D. Wright, *Appl. Phys. Lett.* **98** (2011) 231911; J. Kalb, F. Spaepen, T. P. Leervad Pedersen, and M. Wuttig, *J. Appl. Phys.* **94** (2003) 4908; S. Davis and G. Gutiérrez, *J. Phys.: Condens. Matter* **23** (2011) 495401
16. V. V. Voronkov and R. Falster, *J. Appl. Phys.* **89** (2001) 5965

## Biography

Robert Morel graduated from the Université de Montréal (CA) and obtained his Ph.D. in 1992. After Post Doctoral stays at the Université Paris-Sud and with the CRNS-Thalès Unité Mixte de Recherches (FR) he joined the French Commissariat à l'énergie atomique in 1998 as a research scientist. He has been mainly involved in the synthesis of nanometric clusters by gas-phase condensation and the studies of their structural and magnetic properties.